

Original Paper

# Fusion to Human Serum Albumin Extends the Circulatory Half-Life and Duration of Antithrombotic Action of the Kunitz Protease Inhibitor Domain of Protease Nexin 2

William P. Sheffield<sup>a,b</sup> Louise J. Eltringham-Smith<sup>b</sup> Varsha Bhakta<sup>a</sup>

<sup>a</sup>Centre for Innovation, Canadian Blood Services, Hamilton, Ontario, <sup>b</sup>Department of Pathology and Molecular Medicine, McMaster University, Hamilton, Ontario, Canada

## Key Words

Coagulation • Thrombosis • Factor XI • Albumin • Protease nexin 2

## Abstract

**Background/Aims:** The Kunitz Protease Inhibitor (KPI) domain of protease nexin 2 (PN2) potentially inhibits coagulation factor XIa. Recombinant KPI has been shown to inhibit thrombosis in mouse models, but its clearance from the murine circulation remains uncharacterized. The present study explored the pharmacokinetic and pharmacodynamic effects of fusing KPI to human serum albumin (HSA) in fusion protein KPIHSA. **Methods:** Hexahistidine-tagged KPI (63 amino acids) and KPIHSA (656 amino acids) were expressed in *Pichia pastoris* yeast and purified by nickel-chelate chromatography. Clearance profiles in mice were determined, as well as the effects of KPI or KPIHSA administration on FeCl<sub>3</sub>-induced vena cava thrombus size or carotid artery time to occlusion, respectively. **Results:** Fusion to HSA increased the mean terminal half-life of KPI by 8-fold and eliminated its interaction with the low density lipoprotein receptor-related protein. KPI and KPIHSA similarly reduced thrombus size and occlusion in both venous and arterial thrombosis models when administered at the time of injury, but only KPI was effective when administered one hour before injury. **Conclusions:** Albumin fusion deflects KPI from rapid *in vivo* clearance without impairing its antithrombotic properties and widens its potential therapeutic window.

© 2018 The Author(s)  
Published by S. Karger AG, Basel

## Introduction

Like most coagulation factors, factor XI (FXI) circulates in plasma as an inactive precursor protein [1]. Cleavage of FXI's Arg<sup>369</sup>-Ile<sup>370</sup> bond, catalyzed either by FXIIa generated through the contact pathway, or by thrombin generated through sequential activation of

William P. Sheffield

Department of Pathology and Molecular Medicine, McMaster University  
HSC 4N66, 1280 Main Street West, Hamilton (Canada)  
E-mail [sheffield@mcmaster.ca](mailto:sheffield@mcmaster.ca)

tissue factor/FVII(a), FIX, and FX, converts FXI to the active serine protease FXIa [1-3]. FXIa activates FIX, providing additional procoagulant impetus when physiological hemostasis must be restored [4]. Neither patients [5] nor mice [6] with genetic deficiency of FXI bleed spontaneously, but instead acquire resistance to thrombosis [7-9]. For these reasons, FXI(a) has become a target for drug development [10]. Although an antisense oligonucleotide agent that reduces FXI mRNA levels and circulating FXI to ~30% of normal, indirectly affecting FXIa concentrations, has been shown to be effective in preventing thrombotic complications after knee replacement [11], efforts to develop agents that directly inhibit FXIa remain at the pre-clinical stage.

Natural physiological inhibitors of FXIa include the serpins protein Z-dependent inhibitor [12],  $\alpha_1$ -proteinase inhibitor [13], C<sub>1</sub>-inhibitor [14], protease nexin 1 [14], antithrombin [15], and  $\alpha_2$ -antiplasmin [14]. These inhibitors demonstrate a wide range of rates of inhibition typically requiring glycosaminoglycans for maximal activity; none inhibit FXIa exclusively or preferentially [14]. In contrast, FXIa is also inhibited in a glycosaminoglycan-independent manner by the Kunitz family inhibitor, protease nexin 2 (PN2) [16-18]. PN2 is an isoform of the amyloid precursor protein ( $\beta$ -APP) that is secreted from the  $\alpha$ -granules of activated platelets [19] and which inhibits its primary target, FXIa, 40- to 500-fold more rapidly than secondary target proteases plasmin, FIXa, FXa, FVIIa/tissue factor, and kallikrein [20].

The anti-FXIa inhibitory domain of PN2 is comprised entirely of the 57 contiguous amino acids located between Glu<sup>289</sup> and Ile<sup>345</sup> of PN2, which form its Kunitz Protease Inhibitor (KPI) domain [21, 22]. Co-crystals of recombinant KPI and the catalytic domain of FXIa revealed that it binds the active site of the protease [23]. Recombinant KPI has been shown to reduce the rate of vascular occlusion or the infarct volume in ferric chloride-induced models of carotid or cerebral artery thrombosis [24], but its clearance rates have not been previously established or modified. We sought to extend the circulatory half-life of KPI by fusing it to human serum albumin.

## Materials and Methods

### *Expression and purification of albumin fusion protein KPIHSA*

Oligodeoxyribonucleotide primers (see Table 1 for sequences) were synthesized by MOBIX Lab (McMaster University central facility, Hamilton, ON, Canada). All DNA amplifications used Phusion heat-stable DNA polymerase according to the manufacturer's instructions (Thermo Fisher Scientific, Waltham, MA, USA). DNA sequences encoding KPI, appropriate for in-frame fusion to a human serum albumin (HSA) cDNA, were assembled using two sequential PCR steps. First, primers PrPKI-1 and ML-08-6225 were used to amplify plasmid pPICZ9ssHV3HSAH6 [25], yielding a 1243 bp product. Following gel purification, this DNA product was amplified again, substituting PrPKI-2 for PrPKI-1. The second 1339 bp amplification product was restricted with XhoI and XbaI and inserted between these sites in pPICZ9ssHSAH<sub>6</sub> [25], yielding pPICZ9ssKPIHSAH<sub>6</sub>. This plasmid contained an open reading frame combining the 80 amino acid prepro- $\alpha$  factor secretory signal sequence (ss), the 57 amino acid KPI domain, a Gly<sub>6</sub>SerMet spacer, the 584 codons of mature HSA, and a C-terminal hexahistidine tag to facilitate purification. Plasmid pPICZ9ssKPIHSAH<sub>6</sub>

**Table 1.** Oligonucleotide sequences used in KPI and KPIHSA expression

Oligonucleotide Name	Oligonucleotide Description	DNA Sequence (5' - 3') & [size]
PrKPI-1	KPI (codons 27-57) sense primer	TGTGCCCCAT TCTTTTACGG CCGATGTGGC GGCAACCGGA ACAACTTTGA CACAGAAGAG TACTGCATGG CCGTGTGTGG CAGCGCCATT GGAGGTGGCG GAGGTGGCTC CATGGAC [117]
PrKPI-2	KPI (codons 1-35) sense primer	TCTCTCGAGA AAAGAGAGGT GTGCTCTGAA CAAGCCGAGA CGGGCCCGTG CCGAGCAATG ATCTCCCGCT GGTACTTTGA TGTGACTGAA GGGGAAGTGTG CCCCATTCTT TTACGGC [117]
ML-08-6225	HSA internal antisense primer downstream of XbaI site	CTCTCCAAGC TGCTCGAAAA GCTC [24]
Pr3	KPI antisense primer to terminate ORF with His6 and termination codons	AGCTTCAATG GTGATGGTGA TGGTGAATTG CGTGCCACA C [41]
Pr4	RAP sense primer to fuse ORF to GST cDNA via NcoI site	GACTCCATGG GACATCATCA TCATCATCAT TACTCGCGGG AGAAGAAC [48]
Pr5	RAP antisense primer to terminate GST-RAP fusion protein via termination codon and EcoRI site	GACTGAATTC TCAGAGTTCG TTGTGCCG [28]

was employed to transform *Pichia pastoris* strain X-33 to Zeocin resistance, transformed cell lines were cultured and induced with methanol, and secreted protein KPIHSA was purified from conditioned media using nickel-chelate affinity chromatography, as previously described [25].

## *Expression and purification of KPI*

To generate a *P. pastoris* expression plasmid directing the expression of unfused KPI, PCR was performed using plasmid pPICZ9ssKPIHSA<sub>6</sub> as the template and primers PrKPI-1 and Pr3. The 360 bp amplification product was restricted with XhoI and EcoRI and the 204 bp restriction product was restricted with, and inserted between, these sites in pPICZ9ssamp [26] to yield pPICZ9ssKPIH<sub>6</sub>. This plasmid was used exactly as described above for pPICZ9ssKPIHSA<sub>6</sub> in directing the expression and purification of recombinant KPI (63 amino acids), comprising the 57 amino acids of KPI and a C-terminal hexahistidine tag.

## *Expression and purification of GST and RAP*

A cDNA encoding human low density lipoprotein receptor-related protein associated protein 1 (LRPAP1, RAP) was purchased from Sino Biological (Beijing, China) and modified by PCR as described above using Pr4 and Pr5. The resulting amplification product was restricted with NcoI and EcoRI and inserted between these sites in pBAD to yield pBAD-RAP, which was used to transform *E. coli* Top10 cells to ampicillin resistance. RAP was purified by nickel-chelate chromatography of bacterial lysates following induction of expression with 0.002% arabinose. Glutathione S-transferase (GST) was purified from cultures of *E. coli* Top10 transformed with pGEX5P and induced with 0.1 mM isopropylthiogalactoside, using affinity chromatography on glutathione-Sepharose as previously described.

## *Mass spectrometry*

A sample of 2.5 mg/ml purified recombinant KPI in sterile double-distilled water was diluted 1:10 in 0.5% formic acid/50% acetonitrile and subjected to time-of-flight (TOF) mass spectrometry using electrospray ionization (ESI) for molecular mass determination by mass spectrometry (ESI/MS) using a Micromass Global Q-TOF Ultima instrument housed at the McMaster Regional Centre for Mass Spectrometry service facility of McMaster University.

## *Inhibition of protease-mediated amidolysis by KPI and KPIHSA*

The velocity of amidolysis of chromogenic substrate S2366 (Instrumentation Laboratory (Lexington, MA, USA) by FXIa was determined using 96-well flat bottom microtiter plates (Immunulon IV, Thermo Fisher Scientific) at 37°C in 20 mM sodium phosphate pH 7.4, 0.1% (w/vol) polyethylene glycol 8000, 100 mM sodium chloride, and 0.1 mM disodium ethylenediaminetetraacetic acid, using wavelength 405 nm and an ELx808 Absorbance Microplate Reader (Biotek, Winooski, VT, USA). Reactions contained 1 nM FXIa, 0 to 2500 μM S2366, and 0 to 20 nM KPI or KPIHSA. Analogous experiments containing factor VIIa (FVIIa) in the presence of tissue factor (TF), factor IXa (FIXa), factor Xa (FXa), or plasmin were conducted using chromogenic substrates Spectrozyme FVIIa and Spectrozyme FIXa (Sekisui Diagnostics GmbH) and S2222 (FXa) and S2251 (plasmin) (Chromogenix). Purified proteases, as well as TF, were purchased from Enzyme Research Laboratories. Inhibitory constants ( $K_i$ ) for the inhibition of all proteases by KPI or KPIHSA were determined from non-linear fit for competitive inhibition of velocity versus substrate plots using GraphPad Prism (GraphPad Software, San Diego, CA, USA).

## *<sup>125</sup>I-labelling of KPI proteins and in vivo clearance studies*

Purified recombinant KPI, KPIHSA, or HSA, all produced in C-terminally hexahistidine-tagged forms in the *P. pastoris* system, as well as human fibrinogen (Enzyme Research Laboratories) were separately iodinated using the Iodogen (Thermo Fisher Scientific) method [27], using sodium <sup>125</sup>I. Radiolabelled protein preparations were dialyzed exhaustively against phosphate-buffered saline. All *in vivo* experiments in this study employed CD1 mice (Charles River, Wilmington, MA, USA) and were approved by the Animal Research Ethics Board of the Faculty of Health Sciences, McMaster University. For clearance studies, mice were injected intravenously with 1 X 10<sup>7</sup> cpm protein-bound KPI, KPIHSA, or HSA, and serial blood samples were taken from the tail vein over time. Acid-bound radioactivity was determined from serial plasma samples. Initial and terminal half-lives were determined using a two compartment model and curve-stripping as previously described [28, 29]. In some experiments radiolabelled protein preparations were combined with purified RAP or GST (0.15 mM final concentration) prior to injection, as previously described [30]. In others, mice were separately injected with 6 X 10<sup>6</sup> cpm protein-bound KPI, KPIHSA, or HSA, and were sacrificed

30 minutes later. Specific organs were excised post-mortem, rinsed in ice-cold saline, and organ-associated radioactivity was determined by  $\gamma$ -counting in a Packard Cobra II counter.

#### *Ferric chloride-treated murine vena cava thrombosis model*

Thrombus formation was induced by topical application of 10% (w/vol)  $\text{FeCl}_3$  on the surgically exposed murine vena cava. Mice were anesthetized with 1.5% isoflurane, the vessel exposed, and recombinant protein (12.7 nmol KPI (90  $\mu\text{g}/\text{mouse}$ ) or KPIHSA (940  $\mu\text{g}/\text{mouse}$ , respectively) or saline vehicle was injected intravenously 2 or 60 minutes prior to application of the  $\text{FeCl}_3$ -saturated filter paper to the vessel, for 3 minutes. Thirty minutes after removal of the filter paper, clots were excised and  $\gamma$ -counted to determine their content of  $^{125}\text{I}$ -fibrin and ( $^{125}\text{I}$ -fibrinogen ( $^{125}\text{I}$ -fibrin(ogen))) by  $\gamma$ -counting as described above [31, 32].

#### *Occlusion of ferric chloride-treated murine carotid arteries*

The time to occlusion (TTO) of surgically exposed murine carotid arteries was determined by following arterial blood flow with a Doppler ultrasound flow meter and a 0.5 mm diameter flow probe (Transonic Systems, Ithaca, NY, USA), following application of  $\text{FeCl}_3$ -saturated filter paper, and determining the earliest time point at which blood flow was reduced to less than 0.10 mL/minute. Filter paper and recombinant protein administration timing was the same as that used in the vena cava model above. Vessels not occluding during the 60 minute observation period had their TTO recorded as 60 minutes. Anesthetic cover in these experiments was provided by intraperitoneal injection of 0.3 ml 2.5% tribromoethanol per mouse.

#### *Statistics*

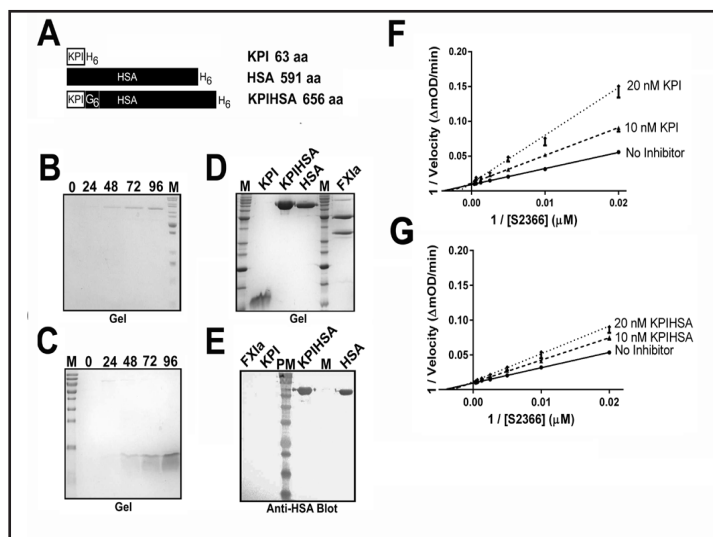
Data is given as the mean  $\pm$  the standard error of the mean (SEM). Statistical analysis was facilitated using GraphPad InStat (GraphPad software). A p value of  $< 0.05$  was taken to indicate statistical significance. For multiple comparisons, data were assessed using ANOVA with post-tests; data sets departing from normal distribution or with dissimilar standard deviations were logarithmically transformed to meet these ANOVA pre-conditions. Paired comparisons employed a two-tailed, unpaired t test, Welch corrected. Additional details are provided in the text and/or figure legends.

## Results

To test whether albumin fusion extended the circulatory half-life of KPI, we designed two recombinant proteins: KPI; and KPIHSA. Both proteins were designed to terminate in a C-terminal hexahistidine tag, for ease of identification and purification, while KPIHSA contained a hexaglycine spacer to provide some spatial separation between the folded fused proteins. The orientation and predicted length of each protein is shown in Fig. 1A, as well as that of previously described recombinant HSA made in the same expression system (HSA, HSAH<sub>6</sub>).

Induction of cultures of *Pichia pastoris* transformed with plasmids specifying the secretion of KPIHSA (Fig. 1B) or KPI (Fig. 1C) led to the appearance of novel 74 kDa and 12 kDa polypeptide species in conditioned media that increased in intensity on stained polyacrylamide gels over 24 to 96 hours. Both putative KPI-related proteins were purified using nickel affinity chromatography that enriched only these major species (Fig. 1D). The putative fusion protein, like recombinant HSA, but not the putative unfused KPI, reacted with anti-HSA antibodies on immunoblots (Fig. 1E); both putative KPI-related proteins reacted with anti-hexahistidine antibodies (data not shown). Positive identification of these proteins was provided by their acting as high affinity competitive inhibitors of FXIa-mediated amidolysis of S2366, as indicated in the Lineweaver-Burke plots shown in Fig. 1F and 1G.  $K_i$  values of  $7 \pm 1$  nM for KPI and  $15 \pm 2$  nM for KPIHSA ( $n=4$ , mean  $\pm$  SEM) were obtained by analysis of these data (Table 2); the difference was statistically significant ( $p = 0.034$  by unpaired t test, Welch corrected). The addition of 5 units/mL standard heparin to kinetic reactions such as those shown in Fig 1F and 1G containing 20 nM KPI or KPIHSA had no effect (data not shown). Because KPI migrated less rapidly on SDS-PAGE in our hands than expected, we verified its mass by ESI/MS; the major peak in the resulting spectrum had a deconvoluted mass of 7090 atomic mass units, a value highly similar to the predicted molecular mass of 7096 Daltons for KPI.

**Fig. 1.** Characterization of fused and unfused forms of KPI. A. Schematic diagrams of recombinant proteins used in this study, depicted in linear form. White boxes show the position of KPI residues 1-56 and black boxes that of HSA residues 1-594. H<sub>6</sub>, hexahistidine tag; G<sub>6</sub>, hexaglycine spacer. The length of the proteins in amino acids (aa) is shown at right. B. Coomassie Blue-stained 12% polyacrylamide SDS gel of conditioned media samples from *P. pastoris* transformed with a plasmid specifying KPIHSA expression. Time of methanol induction in hours is shown above the lanes. M, molecular weight standards (in kDa): 200; 150; 120; 100; 85; 70; 60; 50 (greater intensity); 40; 30; 25; and 20. C. As in B, but for *P. pastoris* transformed with a plasmid specifying KPI expression. D. Stained gel of purified proteins identified above the lanes. E. Immunoblotted replica of the gel shown in D, probed with anti-HSA antibodies, with the addition of PM, pre-stained molecular weight markers. F. Lineweaver-Burke plot of the reciprocal of reaction velocity versus the reciprocal of chromogenic substrate S2366 concentration for inhibition of FXIa-mediated amidolysis by KPI. Data points are arithmetic means  $\pm$  SEM ( $n=5$ ), with downward pointing error bars. G, as in F but for KPIHSA.



Having noted a 2-fold difference in the  $K_i$  values for inhibition of FXIa by KPI versus KPIHSA, we next compared the kinetics of enzyme inhibition of the two forms of KPI for other serine proteases. As expected,  $K_i$  values for inhibition of these other proteases by KPI were increased 14- to 340-fold over the corresponding values for inhibition of FXIa. However, in contrast to the results obtained with FXIa, no significant difference was found between the  $K_i$  values for KPI versus those of KPIHSA for FVIIa, FIXa, FXa, or plasmin inhibition (Table 2).

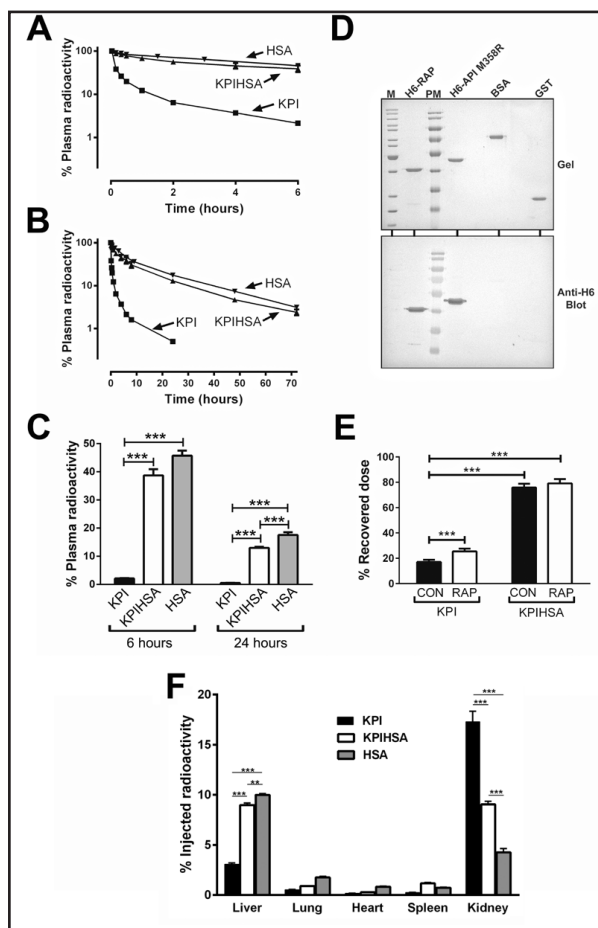
**Table 2.** Inhibitory constants for inhibition of different proteases by KPI or KPIHSA. <sup>a</sup>Values are means  $\pm$  SEM,  $n=4$ . P values were determined using two-tailed, unpaired t test with Welch correction applied

Protease	Inhibitory constant ( $K_i$ ) (nM) <sup>a</sup>		p value
	KPI	KPIHSA	
FXIa	7 $\pm$ 1	15 $\pm$ 2	0.034
FVIIa	2400 $\pm$ 500	2500 $\pm$ 200	0.81
FIXa	1100 $\pm$ 200	1190 $\pm$ 60	0.99
FXa	1400 $\pm$ 200	1100 $\pm$ 300	0.44
Plasmin	100 $\pm$ 10	90 $\pm$ 10	0.40

The clearance profile of KPI in mice diverged from that of KPIHSA or HSA within minutes of injection (Fig. 2A and 2B); after 30 minutes, only  $17 \pm 1\%$  of the initial dose of KPI remained in the circulation, significantly less than either KPIHSA ( $77 \pm 2\%$ ,  $p < 0.05$  vs. KPI) or HSA ( $80 \pm 2\%$ ,  $p < 0.01$  vs. KPI) ( $n=6-12$ ), which did not differ between themselves. The same order of protein clearance (KPI >> KPIHSA = HSA) was apparent at 6 hours post-injection (Fig. 2C), while by 24 hours post-injection the more rapid clearance of KPIHSA than HSA had become statistically significant (KPI >> KPIHSA > HSA). Resolution of clearance curves using a two compartment model was used to calculate initial ( $\alpha$ ) and terminal ( $\beta$ ) half-lives, as shown in Table 3. Fusion to albumin significantly prolonged the mean  $t_{1/2\alpha}$  of KPI 8.5-fold, but KPIHSA remained 2.3-fold more rapidly cleared than HSA. Similarly, the mean  $t_{1/2\beta}$  of KPI was significantly prolonged 6.5-fold via fusion, but it remained 1.1-fold less rapidly cleared



**Fig. 2.** Comparison of clearance profiles of recombinant proteins in mice. A. The percentage of protein-bound radioactivity remaining in the circulation of mice intravenously injected with  $^{125}\text{I}$ -labelled proteins (identified on the graph, with arrows to relevant curves) is shown, versus time after injection. Data points are arithmetic means  $\pm$  SEM (from three groups of mice,  $n=6$  mice per group), with downward pointing error bars (not visible in most cases due to logarithmic scale and smaller size than graph symbols). Each data point was normalized to the radioactivity present in the initial 2 minute sample of the mouse. B. As in A, but for a longer time period post-injection. C. Residual radioactivity 6 (left) or 24 hours (right) after injection from curves shown in A and B. Arithmetic means  $\pm$  SEM ( $n=9$  [KPI], 12 [KPIHSA], or 6 [HSA]). \*\*\* ( $p<0.001$ ) indicates significant difference between the groups (identified on the x axis) linked by horizontal lines (ANOVA). D. Upper panel, Coomassie Blue-stained 10% polyacrylamide SDS gel of purified proteins identified above the lanes. M, markers (same as Fig. 1) and PM (prestained molecular mass markers, 180, 130, 95, 72, 55, 43, 34, and 26 kDa). Lower panel, immunoblotted replicate gel probed with anti-hexahistidine antibodies. E. The percentage of the protein-bound radioactive dose recovered 2 minutes post injection for KPI (left columns) or KPIHSA (right columns) co-injected with control protein GST (CON, black bars) or RAP (white bars) is shown (arithmetic means  $\pm$  SEM,  $n=6$ ). \*\*\* ( $p<0.001$ ) indicates significant difference between the groups (identified on the x axis) linked by horizontal lines (ANOVA). F. The percentage of the total radioactive dose recovered 30 minutes post-injection for KPI (grey bars), KPIHSA (white bars), or HSA (black bars) is shown for each of five organs identified on the x axis (arithmetic means  $\pm$  SEM,  $n=6$ ). \*\* ( $p<0.01$ ) and \*\*\* ( $p<0.001$ ) indicates significant difference between the groups, for liver or kidney, for groups at the outer limits of the horizontal lines above the graphs (ANOVA). Only data from organs with  $>1\%$  KPI distribution (liver and kidneys) were evaluated statistically. Five organ samples were taken from each mouse of groups of six.



for KPI (left columns) or KPIHSA (right columns) co-injected with control protein GST (CON, black bars) or RAP (white bars) is shown (arithmetic means  $\pm$  SEM,  $n=6$ ). \*\*\* ( $p<0.001$ ) indicates significant difference between the groups (identified on the x axis) linked by horizontal lines (ANOVA). F. The percentage of the total radioactive dose recovered 30 minutes post-injection for KPI (grey bars), KPIHSA (white bars), or HSA (black bars) is shown for each of five organs identified on the x axis (arithmetic means  $\pm$  SEM,  $n=6$ ). \*\* ( $p<0.01$ ) and \*\*\* ( $p<0.001$ ) indicates significant difference between the groups, for liver or kidney, for groups at the outer limits of the horizontal lines above the graphs (ANOVA). Only data from organs with  $>1\%$  KPI distribution (liver and kidneys) were evaluated statistically. Five organ samples were taken from each mouse of groups of six.

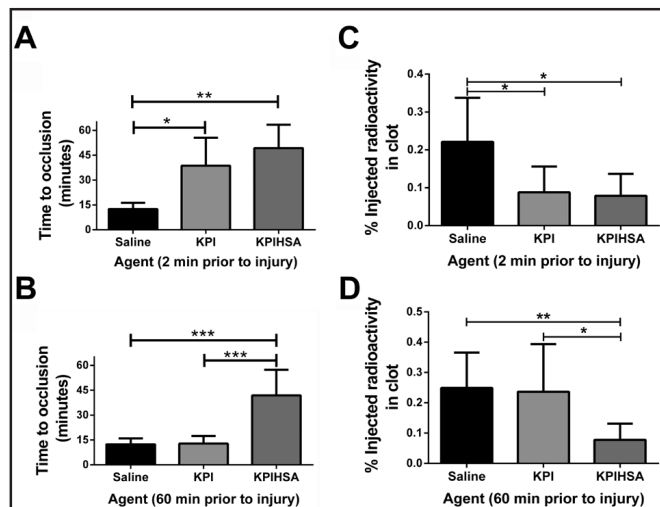
than HSA. Both clearance phases combined yielded a significantly increased area under the observed clearance curve (AUC) of 18-fold for KPIHSA versus KPI, which remained 1.1-fold less than the HSA AUC.

Previous *in vitro* studies have shown that PN2 and/or PN2-protease complexes are internalized by the a cellular receptor called the lipoprotein receptor-related protein (LRP) [33, 34]; accord-

**Table 3.** Clearance profiles of KPI, KPIHSA, and HSA in mice<sup>a</sup>. <sup>a</sup>Results are means  $\pm$  SD,  $n=6$ . Initial ( $\alpha$ ) and terminal ( $\beta$ ) half-lives ( $t_{1/2}$ ) are shown. \*\*\* indicates  $p < 0.001$  versus KPI value; + or +++ indicate,  $p < 0.05$  or  $< 0.001$  versus KPIHSA value by ANOVA with post-tests

	$t_{1/2\alpha}$ (hours)	$t_{1/2\beta}$ (hours)	Area under the observed clearance curve (AUC; %-hours)
KPI	$0.13 \pm 0.02$	$2.6 \pm 0.3$	$0.50 \pm 0.09$
KPIHSA	$1.1 \pm 0.3^{***}$	$17 \pm 1^{***}$	$8.8 \pm 0.4^{***}$
HSA	$2.5 \pm 0.8^{***, +}$	$19 \pm 1^{***, +++}$	$11 \pm 1^{***, +++}$

**Fig. 3.** Antithrombotic effects of KPI or KPIHSA in mice. A. Time to occlusion of murine carotid arteries treated with ferric chloride and with agents identified on the x axis 2 minutes prior to injury. Bars are arithmetic means  $\pm$  SEM (n=6 mice per group, dosed with 12.7 nmol KPI (90  $\mu$ g/mouse) or KPIHSA (940  $\mu$ g/mouse, respectively). B. As in A, but treated with agents 60 minutes prior to injury. C. Percentage of injected  $^{125}$ I-fibrinogen found in murine vena cava clots following treatment with ferric chloride and with agents identified on the x axis 2 minutes prior to injury. Bars are arithmetic means  $\pm$  SEM (n=9). D. As in C, but treated with agents 60 minutes prior to injury. \* (p<0.05), \*\* (p<0.01), \*\*\* (p<0.001) indicates significant difference between the groups (identified on the x axis) linked by horizontal lines (ANOVA).



ingly, we sought to determine if the LRP antagonist RAP (also called LRPAP1) affected KPI or KPIHSA clearance *in vivo*. Recombinant RAP was produced in a bacterial expression system and purified to near homogeneity, as was unrelated control protein GST (Fig. 2D, upper panel); RAP, but not GST, reacted with anti-hexahistidine antibodies due to the planned presence of a hexahistidine tag in the former, but not the latter protein (Fig. 2, lower panel). Recovery of injected radiolabelled protein two minutes after injection was significantly greater for KPI, but not KPIHSA, following administration of RAP than following administration of an identical dose of control protein GST (Fig. 2E).

Fusion to albumin changed not only the clearance behaviour of KPI but also its organ distribution (Fig. 2F). Of five organs sampled 30 minutes post-injection, KPI was predominantly found in the kidneys, to a significantly (1.9-fold) greater extent than KPI; this differential localization was even more pronounced with respect to HSA (4.1-fold). Fusion to albumin also significantly redirected KPI to the liver, as evidenced by the detection of 2.9-fold more KPIHSA than KPI in that organ, versus 3.2-fold more HSA (both changes significant).

The effectiveness of KPI and KPIHSA as antithrombotic agents was tested *in vivo* in anesthetized mice with surgically exposed carotid arteries (Fig. 3A or 3B) or vena cava (Fig. 3C and 3D) treated with ferric chloride. Both KPI-related proteins significantly prolonged the time to arterial occlusion (Fig. 3A) or decreased the size of the venous clot (Fig. 3C) when administered two minutes prior to induction of thrombosis, at equimolar doses, versus saline vehicle controls. However, when the time between recombinant protein administration and induction of thrombosis was increased to 60 minutes, KPI lost its antithrombotic activity in either arterial or venous models, while KPIHSA continued to exert its antithrombotic effects in both settings (Fig. 3B and 3D).

## Discussion

The present study tested two hypotheses: that KPI would exhibit rapid *in vivo* clearance from the circulation after injection; and that fusion of KPI to HSA would increase its circulatory half-life and duration of antithrombotic action. With respect to the first hypothesis, and as predicted by Wu et al [24], KPI was rapidly removed from the murine circulation after intravenous injection. KPI clearance resembled that of other small proteins less than 80 amino acids in length such as hirudin [25, 35] or barbourin [36], which are characterized by rapid renal losses without reabsorption. Specifically with respect to recombinant hexahistidine-tagged hirudin variant 3 (HV3), we previously noted that ~90%

of the radiolabeled dose was lost from the murine circulation within one hour of injection, a profile highly similar to that we observed for KPI in the current study [25]. Fusion to albumin slowed both the rapid and slower phases of KPI's biphasic clearance by 6.5- to 8.5-fold, providing a clear pharmacokinetic enhancement. The prolongation of KPI residence time in the circulation afforded by albumin fusion also correlated with prolonged antithrombotic action. Administration of KPI one hour before induction of thrombosis eliminated its antithrombotic effects, consistent with its expected disappearance from the circulation. KPI had previously been demonstrated to reduce the size of carotid artery thrombi or ischemic brain damage arising from occlusion of the middle cerebral artery in mice, either in isolated form [24] or when present in PN2 [37]. Our results are therefore consistent with these previous findings and extend them into the venous thrombosis setting.

Although fusion to albumin prolonged the rate of KPI clearance, it did not equalize it to that of recombinant HSA in mice. There are at least two potential explanations for this observation. Albumin fusion is thought to extend clearance of fused proteins by deflection from glomerular filtration and through recycling after endocytosis mediated by the neonatal Fc receptor (FcRn) [38]. A fusion protein could fail to acquire the full, slowly cleared phenotype of albumin due either to retention of binding sites for clearance receptors or by obscuring the FcRn binding sites on albumin by steric hindrance or allosteric effects [39]. KPI cleared less rapidly when co-injected into mice with the LRP antagonist RAP, but RAP had no significant effect on KPIHSA clearance when co-administered with the fusion protein. It therefore seems more likely that the attachment of KPI to HSA obscured some determinant on the HSA surface partially mediating FcRn-dependent recycling. HSA has three domains, and mutagenic studies using one- or two-domain recombinant fragments of HSA have shown a principal human FcRn binding site in C-terminal domain III, but also some contribution of N-terminal domain I [40]. The latter region might be affected by attachment of KPI to the N-terminus of recombinant HSA. It should be noted that HSA is not recognized as effectively by murine FcRn as murine serum albumin, and this incompatibility contributes to the shorter half-life of HSA in mice than in humans [41]. Andersen et al. found a terminal half-life for HSA in mice of 21 hours, compared to 11 hours in this study; both values fall far short of the 19 day half-life of HSA in humans [40]. The comparatively minor difference between the two HSA observed half-lives in mice could have arisen due to differences in detection methods (unlabelled or radiolabelled), expression systems (*Saccharomyces cerevisiae* or *Pichia pastoris*), or affinity tags (myc epitope or hexahistidine).

Fusion of KPI to HSA not only conferred the bulk of HSA's slowly cleared phenotype on KPI, it also left most of the affinity of KPI for FXIa intact in KPIHSA. This retention was demonstrated by the minor 2.1-fold increase in  $K_i$  of KPIHSA for FXIa compared to that of KPI.  $K_i$  values for other serine proteases less rapidly inhibited by KPI (e.g. plasmin) were unaffected by albumin fusion. Co-crystallization of KPI with the catalytic domain of FXIa revealed tight contacts between two KPI loops (residues 11-20 and 34-38) linked by a disulphide bond between Cys14 and Cys38: 11TGPCRAMISR20 (P5-P5'); and 34FYGGC38 [23]. The C-terminus of KPI is freely accessible in the structure, suggesting that the minor reduction in affinity of KPIHSA for FXIa likely arises from conformational changes transmitted through the KPI chain, as opposed to steric hindrance involving possible clashes between the HSA moiety of the fusion protein and FXIa. It is also possible that this effect could be minimized by optimization of the hexaglycine spacer found between the KPI and HSA domains of KPIHSA; previous improvements to the activity of a coagulation factor IX HSA fusion protein were achieved by substituting a longer spacer for a shorter one [42]. The  $K_i$  of recombinant KPI for FXIa has previously been reported as 0.45 nM, substantially lower than determined in this study, but that form of KPI differed from that we employed in containing three additional PN2 residues, lacked a hexahistidine addition, and was assessed kinetically using different methodology [43].

Our *in vitro* results confirm previous observations that KPI is not absolutely specific for FXIa, and extend them by showing that this inhibitory profile is mirrored in fusion protein KPIHSA. The ability of both KPI and KPIHSA to inhibit other coagulation proteins raises the



possibility that their antithrombotic activity does not derive from the inhibition of FXIa alone. While this possibility cannot be absolutely excluded, it is unlikely for several reasons. Firstly, *in vitro* results from both this study and previously published work suggest that KPI inhibits FXIa much more rapidly than FXa or FIXa. Their zymogen precursor proteins, FIX and FX, are present at similar concentrations in plasma [44]; assuming that similar amounts of activated coagulation proteins are generated *in vivo* in each case in clot formation, KPI would inhibit FXIa long before having an effect on the other two proteases. The same logic applies to FVIIa, but to a greater extent, in that the plasma concentration of zymogen FVII is 10- to 20-fold lower than that of FXI, FX, or FIX. Secondly, of the tested proteases, plasmin is the closest second to FXIa with respect to its speed of inactivation by KPI or KPIHSA. If KPI inhibited plasmin it would promote thrombus formation or thrombotic occlusion, not counteract these processes. Thus, even in the unlikely event that KPI or KPIHSA significantly inhibit plasmin *in vivo*, this would not negate the primary effect of these proteins as FXIa inhibitors.

Current interest in inhibiting FXIa is high [10]. To date, the only anti-FXI strategy that has been tested in clinical trials is reduction of FXI mRNA and protein via antisense oligonucleotide administration [11]. In preclinical models, several small peptidomimetic candidate drugs and several anti-FXI monoclonal antibodies have shown some promise as antithrombotic agents [45]. KPI is a human polypeptide, naturally occurring within the context of soluble, non-amyloidogenic isoforms of PN2 (also known as the amyloid precursor protein), that would not be expected to be immunogenic or toxic. Here we have demonstrated that KPI linked to HSA, a human polypeptide with an excellent safety profile, both as a stand-alone drug and as a fusion partner, retains its efficacy as an antithrombotic agent in a prolonged manner. In mice, KPI demonstrates a clearance profile with and without HSA fusion very similar to that of hirudin variant 3. We found an approximate 10-fold extension of terminal half-life of HV3 in mice for HV3HSA fusion protein [25] and a 160-fold extension in rabbits for a homologous HV3-rabbit serum albumin fusion protein [35]. It is therefore likely that KPIHSA will demonstrate even larger increments in circulatory half-life in non-murine systems.

One limitation of our study is that we lacked the opportunity or resources to test KPIHSA in a genetically engineered mouse model in which the  $\beta$ -APP gene has been ablated [46].  $\beta$ -APP knockout mice were shown to exhibit a significant, ~25% reduction in TTO of carotid arteries treated with Rose Bengal dye and laser light. Based on our results in this study, we predict that either KPI or KPIHSA would restore TTO to wild-type levels if provided at doses similar to those we employed in the  $\text{FeCl}_3$ -treated carotid artery thrombosis model in sufficiently powered experiments.

## Conclusion

KPIHSA could therefore be used in both murine and non-murine animal models to explore further the pathophysiological consequences of FXIa inhibition, and could one day join the ranks of clinically employed HSA fusion proteins, such as those engineered with coagulation factor IX and glucagon-like peptide-1 agonist partners.

## Acknowledgements

This study was made possible by Grant-In-Aid G-15-0009117 from the Heart and Stroke Foundation of Canada to WPS. The authors thank Dr. Syed M. Qadri (Canadian Blood Services and McMaster University) for helpful discussions and suggestions. WPS and VB are members of the Canadian Blood Services Centre for Innovation, which receives funding from Health Canada, a department of the federal government of Canada. This article must therefore, as a condition of funding, contain the statement, "The views expressed herein do not necessarily represent the views of the federal government [of Canada]."

## Disclosure Statement

No conflict of interest exists.

## References

- 1 Bouma BN, Griffin JH: Human blood coagulation factor XI. Purification, properties, and mechanism of activation by activated factor XII. *J Biol Chem* 1977;252:6432-6437.
- 2 Naito K, Fujikawa K: Activation of human blood coagulation factor XI independent of factor XII. Factor XI is activated by thrombin and factor XIa in the presence of negatively charged surfaces. *J Biol Chem* 1991;266:7353-7358.
- 3 Gailani D, Broze GJ, Jr.: Factor XI activation in a revised model of blood coagulation. *Science* 1991;253:909-912.
- 4 Emsley J, McEwan PA, Gailani D: Structure and function of factor XI. *Blood* 2010;115:2569-2577.
- 5 Gomez K, Bolton-Maggs P: Factor XI deficiency. *Haemophilia* 2008;14:1183-1189.
- 6 Gailani D, Lasky NM, Broze GJ, Jr.: A murine model of factor XI deficiency. *Blood Coagul Fibrinolysis* 1997;8:134-144.
- 7 Rosen ED, Gailani D, Castellino FJ: FXI is essential for thrombus formation following FeCl<sub>3</sub>-induced injury of the carotid artery in the mouse. *Thromb Haemost* 2002;87:774-776.
- 8 Wang X, Cheng Q, Xu L, Feuerstein GZ, Hsu MY, Smith PL, Seiffert DA, Schumacher WA, Ogletree ML, Gailani D: Effects of factor IX or factor XI deficiency on ferric chloride-induced carotid artery occlusion in mice. *J Thromb Haemost* 2005;3:695-702.
- 9 Preis M, Hirsch J, Kotler A, Zoabi A, Stein N, Rennert G, Saliba W: Factor XI deficiency is associated with lower risk for cardiovascular and venous thromboembolism events. *Blood* 2017;129:1210-1215.
- 10 Weitz JI: Factor XI and factor XII as targets for new anticoagulants. *Thromb Res* 2016;141:S40-45.
- 11 Buller HR, Bethune C, Bhanot S, Gailani D, Monia BP, Raskob GE, Segers A, Verhamme P, Weitz JI, Investigators F-AT: Factor XI antisense oligonucleotide for prevention of venous thrombosis. *N Engl J Med* 2015;372:232-240.
- 12 Tabatabai A, Fiehler R, Broze GJ, Jr.: Protein Z circulates in plasma in a complex with protein Z-dependent protease inhibitor. *Thromb Haemost* 2001;85:655-660.
- 13 Scott CF, Schapira M, James HL, Cohen AB, Colman RW: Inactivation of factor XIa by plasma protease inhibitors: predominant role of alpha 1-protease inhibitor and protective effect of high molecular weight kininogen. *J Clin Invest* 1982;69:844-852.
- 14 Wuillemin WA, Eldering E, Citarella F, de Ruig CP, ten Cate H, Hack CE: Modulation of contact system proteases by glycosaminoglycans. Selective enhancement of the inhibition of factor XIa. *J Biol Chem* 1996;271:12913-12918.
- 15 Scott CF, Schapira M, Colman RW: Effect of heparin on the inactivation rate of human factor XIa by antithrombin-III. *Blood* 1982;60:940-947.
- 16 Kitaguchi N, Takahashi Y, Tokushima Y, Shiojiri S, Ito H: Novel precursor of Alzheimer's disease amyloid protein shows protease inhibitory activity. *Nature* 1988;331:530-532.
- 17 Smith RP, Higuchi DA, Broze GJ, Jr.: Platelet coagulation factor XIa-inhibitor, a form of Alzheimer amyloid precursor protein. *Science* 1990;248:1126-1128.
- 18 Van Nostrand WE, Schmaier AH, Farrow JS, Cunningham DD: Protease nexin-II (amyloid beta-protein precursor): a platelet alpha-granule protein. *Science* 1990;248:745-748.
- 19 Van Nostrand WE, Schmaier AH, Farrow JS, Cines DB, Cunningham DD: Protease nexin-2/amyloid beta-protein precursor in blood is a platelet-specific protein. *Biochem Biophys Res Commun* 1991;175:15-21.
- 20 Navaneetham D, Sinha D, Walsh PN: Mechanisms and specificity of factor XIa and trypsin inhibition by protease nexin 2 and basic pancreatic trypsin inhibitor. *J Biochem* 2010;148:467-479.
- 21 Ponte P, Gonzalez-DeWhitt P, Schilling J, Miller J, Hsu D, Greenberg B, Davis K, Wallace W, Lieberburg I, Fuller F: A new A4 amyloid mRNA contains a domain homologous to serine proteinase inhibitors. *Nature* 1988;331:525-527.
- 22 Badellino KO, Walsh PN: Protease nexin II interactions with coagulation factor XIa are contained within the Kunitz protease inhibitor domain of protease nexin II and the factor XIa catalytic domain. *Biochemistry* 2000;39:4769-4777.
- 23 Navaneetham D, Jin L, Pandey P, Strickler JE, Babine RE, Abdel-Meguid SS, Walsh PN: Structural and mutational analyses of the molecular interactions between the catalytic domain of factor XIa and the Kunitz protease inhibitor domain of protease nexin 2. *J Biol Chem* 2005;280:36165-36175.

- 24 Wu W, Li H, Navaneetham D, Reichenbach ZW, Tuma RF, Walsh PN: The kunitz protease inhibitor domain of protease nexin-2 inhibits factor XIa and murine carotid artery and middle cerebral artery thrombosis. *Blood* 2012;120:671-677.
- 25 Sheffield WP, Eltringham-Smith LJ, Gataiance S, Bhakta V: A long-lasting, plasmin-activatable thrombin inhibitor aids clot lysis *in vitro* and does not promote bleeding *in vivo*. *Thromb Haemost* 2009;101:867-877.
- 26 Sheffield WP, Smith IJ, Syed S, Bhakta V: Prolonged *in vivo* anticoagulant activity of a hirudin-albumin fusion protein secreted from *Pichia pastoris*. *Blood Coagul Fibrinolysis* 2001;12:433-443.
- 27 Fraker PJ, Speck JC, Jr.: Protein and cell membrane iodinations with a sparingly soluble chloroamide, 1, 3,4, 6-tetrachloro-3a,6a-diphrenylglycoluril. *Biochem Biophys Res Commun* 1978;80:849-857.
- 28 Sheffield WP, Mamdani A, Hortelano G, Gataiance S, Eltringham-Smith L, Begbie ME, Leyva RA, Liaw PS, Ofosu FA: Effects of genetic fusion of factor IX to albumin on *in vivo* clearance in mice and rabbits. *Br J Haematol* 2004;126:565-573.
- 29 Begbie ME, Mamdani A, Gataiance S, Eltringham-Smith LJ, Bhakta V, Hortelano G, Sheffield WP: An important role for the activation peptide domain in controlling factor IX levels in the blood of haemophilia B mice. *Thromb Haemost* 2005;94:1138-1147.
- 30 Saenko EL, Yakhyayev AV, Mikhailenko I, Strickland DK, Sarafanov AG: Role of the low density lipoprotein-related protein receptor in mediation of factor VIII catabolism. *J Biol Chem* 1999;274:37685-37692.
- 31 Sheffield WP, Eltringham-Smith LJ: Incorporation of albumin fusion proteins into fibrin clots *in vitro* and *in vivo*: comparison of different fusion motifs recognized by factor XIIIa. *BMC Biotechnol* 2011;11:127.
- 32 Sheffield WP, Eltringham-Smith LJ, Bhakta V, Gataiance S: Reduction of thrombus size in murine models of thrombosis following administration of recombinant alpha1-proteinase inhibitor mutant proteins. *Thromb Haemost* 2012;107:972-984.
- 33 Kounnas MZ, Moir RD, Rebeck GW, Bush AI, Argraves WS, Tanzi RE, Hyman BT, Strickland DK: LDL receptor-related protein, a multifunctional ApoE receptor, binds secreted beta-amyloid precursor protein and mediates its degradation. *Cell* 1995;82:331-340.
- 34 Knauer ME, Orlando RA, Glabe CG: Cell surface APP751 forms complexes with protease nexin 2 ligands and is internalized via the low density lipoprotein receptor-related protein (LRP). *Brain Res* 1996;740:6-14.
- 35 Syed S, Schuyler PD, Kulczycky M, Sheffield WP: Potent antithrombin activity and delayed clearance from the circulation characterize recombinant hirudin genetically fused to albumin. *Blood* 1997;89:3243-3252.
- 36 Marques JA, George JK, Smith IJ, Bhakta V, Sheffield WP: A barbourin-albumin fusion protein that is slowly cleared *in vivo* retains the ability to inhibit platelet aggregation *in vitro*. *Thromb Haemost* 2001;86:902-908.
- 37 Xu F, Davis J, Hoos M, Van Nostrand WE: Mutation of the Kunitz-type proteinase inhibitor domain in the amyloid beta-protein precursor abolishes its anti-thrombotic properties *in vivo*. *Thromb Res* 2017;155:58-64.
- 38 Chaudhury C, Mehnaz S, Robinson JM, Hayton WL, Pearl DK, Roopenian DC, Anderson CL: The major histocompatibility complex-related Fc receptor for IgG (FcRn) binds albumin and prolongs its lifespan. *J Exp Med* 2003;197:315-322.
- 39 Sheffield WP: Modification of clearance of therapeutic and potentially therapeutic proteins. *Curr Drug Targets Cardiovasc Haematol Disord* 2001;1:1-22.
- 40 Andersen JT, Dalhus B, Cameron J, Daba MB, Plumridge A, Evans L, Brennan SO, Gunnarsen KS, Bjoras M, Sleep D, Sandlie I: Structure-based mutagenesis reveals the albumin-binding site of the neonatal Fc receptor. *Nat Commun* 2012;3:610.
- 41 Andersen JT, Daba MB, Berntzen G, Michaelsen TE, Sandlie I: Cross-species binding analyses of mouse and human neonatal Fc receptor show dramatic differences in immunoglobulin G and albumin binding. *J Biol Chem* 2010;285:4826-4836.
- 42 Metzner HJ, Weimer T, Kronthaler U, Lang W, Schulte S: Genetic fusion to albumin improves the pharmacokinetic properties of factor IX. *Thromb Haemost* 2009;102:634-644.
- 43 Wagner SL, Siegel RS, Vedvick TS, Raschke WC, Van Nostrand WE: High level expression, purification, and characterization of the Kunitz-type protease inhibitor domain of protease nexin-2/amyloid beta-protein precursor. *Biochem Biophys Res Commun* 1992;186:1138-1145.
- 44 Favalaro EJ, Soltani S, McDonald J, Grezchnik E, Easton L: Cross-laboratory audit of normal reference ranges and assessment of ABO blood group, gender and age on detected levels of plasma coagulation factors. *Blood Coagul Fibrinolysis* 2005;16:597-605.
- 45 Chen Z, Seiffert D, Hawes B: Inhibition of Factor XI activity as a promising antithrombotic strategy. *Drug Discov Today* 2014;19:1435-1439.
- 46 Xu F, Davis J, Miao J, Previti ML, Romanov G, Ziegler K, Van Nostrand WE: Protease nexin-2/amyloid beta-protein precursor limits cerebral thrombosis. *Proc Natl Acad Sci U S A* 2005;102:18135-18140.